



# Covalently crosslinked organophosphorous derivatives-chitosan hydrogel as a drug delivery system for oral administration of camptothecin



Mayte Martínez-Martínez<sup>a</sup>, Guillermo Rodríguez-Berna<sup>b</sup>, Marival Bermejo<sup>a</sup>,  
Isabel Gonzalez-Alvarez<sup>a</sup>, Marta Gonzalez-Alvarez<sup>a,\*</sup>, Virginia Merino<sup>c</sup>

<sup>a</sup> Dpto. de Ingeniería, Área Farmacia y Tecnología Farmacéutica, Universidad Miguel Hernández, Carretera Alicante-Valencia km. 87, 03550, San Juan, Alicante, Spain

<sup>b</sup> Instituto Mixto de Tecnología Química, Universidad Politécnica de Valencia-Consejo Superior de Investigaciones Científicas (UPV-CSIC), Avd. de los Naranjos s/n, 46006 Valencia, Spain

<sup>c</sup> Instituto Interuniversitario de Investigación de Reconocimiento Molecular y Desarrollo Tecnológico (IDM), Universitat Politècnica de València, Universitat de València, Dpto. de Farmacia y Tecnología Farmacéutica y Parasitología, Vicente Andrés Estelles s/n, Burjassot, Valencia, Spain

## ARTICLE INFO

### Keywords:

Camptothecin  
Hydrogel  
Drug delivery  
Oral administration  
Chemotherapy  
Mucoadhesivity

## ABSTRACT

Hydrogels are widely studied as drug delivery system. In this work we propose the employment of tetrakis (hydroxymethyl)phosphonium chloride as crosslinking agent to obtain covalent hydrogels based on chitosan. These hydrogels are obtained by Mannich reaction between the amino groups of chitosan with the hydroxymethyl groups of the crosslinker molecule. They show a pH sensitive second order swelling kinetic, have low toxicity, are biocompatible, mucoadhesive and allow a modified release of the encapsulated drug, camptothecin, for 48 h. This antitumor drug has been studied as a drug of interest to develop oral chemotherapy administration strategies. According to the obtained results, oral administration of camptothecin through hydrogels would provide low concentrations of drug at the absorption site, avoiding carrier saturation and reducing its intestinal toxicity.

## 1. Introduction

Oral chemotherapy is one of the great challenges in cancer treatment, but only a few drugs have achieved promising results in this field. It is well-known that oral route of administration of chemotherapeutics presents many advantages, as it provides a sustained exposure of cancer cells to low drug concentrations, which implies greater efficacy and fewer adverse effects. It is known that a long-time exposure of cancer cells to low drug concentrations implies better effects than a pulsed supply of the drug at a high concentration [1,2]. In fact, some clinical studies found that oral chemotherapy had lower toxicity and clinical outcomes comparable or even better than intravenous administration [3]. Additional benefits of oral chemotherapy are lower cost, flexibility in dosing schedule and a better patient convenience resulting in improved quality of life [1–4].

Camptothecin (CPT) is considered one of the most potent antitumor compounds known, with a broad spectrum of cytotoxicity in several tumor cell lines. CPT has the maximal activity in the S-phase of the cell cycle and its union to the DNA-topoisomerase I complex is reversible

[5], consequently a prolonged exposure is required for optimal efficacy [6]. Thus, maintained plasma concentrations following continuous oral delivery would ensure therapeutic efficacy of CPT.

However, the full therapeutic potential of CPT is extremely limited because of its poor aqueous solubility and the rapid inactivation to the pharmacologically inactive carboxylate form, due to the lactone hydrolysis at physiological pH [7]. Different approaches have been utilized to improve the solubility and the stability issues of the alkaloid [8–10], but in most cases the incorporation of the CPT into the delivery system is quite inefficient and requires a prodrug form to improve the loading and control the release. Moreover, the intestinal permeability is also a relevant factor to take into account for oral administration. Despite CPT permeability has been previously studied [11,12], the classification of CPT according to Biopharmaceutical Classification System (BCS) remains unclear.

The physicochemical and biological features of hydrogels have attracted the interest of a broad range of biomedical applications such as tissue engineering and controlled drug delivery systems [13]. Hydrogels can be considered a good option to administrate CPT orally for

*Abbreviations:* CPT, camptothecin; THP, tetrakis(hydroxymethyl)phosphonium chloride; SEM, scanning electron microscopy; LMW, chitosan low molecular weight; MMW, chitosan medium molecular weight; HMW, chitosan high molecular weight; DD, deacetylation degree

\* Corresponding author at: Edificio Muhammad Al-Shafra, Campus UMH, Carretera Alicante Valencia km 87, 03550, San Juan de Alicante, Alicante, Spain.

E-mail address: [marta.gonzalez@umh.es](mailto:marta.gonzalez@umh.es) (M. Gonzalez-Alvarez).

<https://doi.org/10.1016/j.ejpb.2019.01.009>

Received 1 November 2018; Received in revised form 8 January 2019; Accepted 11 January 2019

Available online 14 January 2019

0939-6411/ © 2019 Published by Elsevier B.V.

several reasons. First, hydrogels provide networks with high water or biological fluids content that offer the possibility to solubilize the drug. Second, its tridimensional structure that mainly includes the anti-tumoral agent inside, protects the intestinal mucosa from the harmful effects of antitumoral until the drug is released. Finally, sustained drug release profiles of hydrogels allow to have prolonged and continuous CPT concentrations at the site of absorption. This is especially advantageous of CPT because it has been described that at low concentrations the transport of CPT is a carrier-mediated active process and passive diffusion accounts for a minor fraction of the transport [11,12]. Therefore, high concentrations of CPT saturate the transporter preventing drug absorption and thereby decreasing its bioavailability.

To date, hydrogels are usually prepared through covalent or non-covalent crosslinking between polymers chains to make robust or reversible networks respectively [14,15]. Covalent hydrogels offer better mechanical properties and improved stability to avoid dissolution, even in extreme pH conditions. Many bifunctional molecules have been used to crosslink the network, including dialdehydes, diglycidyl ether, diisocyanate, diacrylate among others [16]. However, most of the crosslinkers used thus far are quite toxic or there is a lack of data regarding their biocompatibility. For example, one of the most commonly used crosslinking agents is glutaraldehyde, which is mutagenic and neurotoxic [17,18]. This has been a challenge in the search for new crosslinking molecules with less toxicity. Genipine is biocompatible and its toxicity is 5000–10,000 times lower than glutaraldehyde [19], although its cost is relatively high.

Tetrakis(hydroxymethyl)phosphonium chloride (THPC), is well known water-soluble commercial organophosphorous compound, relatively inexpensive, previously reported such as immobilizing agent, organic ligand in coordination chemistry, flame retardant for cotton textiles [20] and, recently, THPC, has proven to be an effective molecule for cell encapsulation [21]. Hydroxymethylphosphines undergo Mannich type condensation reactions in soft conditions with primary and secondary amine containing compounds [21], giving a very stable aminomethylphosphine crosslink against the hydrolyzable imine bond formed by aldehydes coupling. Furthermore, due to the tetra-functionality of the organophosphorous compounds and their high reactivity in aqueous environment we hypothesized an *in situ* gelation process allowing to obtain a hydrogel system.

On the other hand, chitosan is a very safe biopolymer, extensively used in controlled drug delivery hydrogel-based systems because its biocompatibility, muco-adhesiveness, non-toxicity and biodegradability [22,16]. Formulations based on chitosan have been designed to delivery drugs or proteins for buccal and oral (gastric, intestinal or colon delivery) administration ways [23–26].

The aim of this study was to develop an oral system with high loading of active 20-(S)-Camptothecin (CPT) and to achieve an optimal delivery profile for oral chemotherapy. For this purpose, chitosan hydrogel was selected such a drug delivery model and THPC as a crosslinker compound.

## 2. Experimental

### 2.1. Materials

Chitosan Low MW (LMW) (deacetylation degree (DD) of 83%, MW = 50–190 kDa), chitosan medium MW (MMW) (deacetylation degree (DD) of 81%, MW = 190–310 kDa), chitosan high MW (HMW) (deacetylation degree (DD) of 95.8%, MW = 310–375 kDa), (S)-(+)-Camptothecin (CPT), metoprolol, 1-methyl-2-pyrrolidinone (NMP), tetrakis(hydroxymethyl)phosphonium chloride solution (THPC), cytocompatibility test LIVE/DEAD®, 3-(4,5-dimethylthiazol-2-yl)-2,5-diphenyltetrazolium bromide (MTT) were purchased from Sigma-Aldrich (Spain). Ultrapure water (Millipore QPAK system) was used to make the solubility test solutions. HBSS (Hanks Balanced Salt Solution), HEPES, PBS (phosphate buffered saline), penicillin G,

streptomycin, fetal bovine serum, trypsin-EDTA, Dubelcco's Modified Eagle's Media-glutamax were purchased from GIBCO.

### 2.2. Camptothecin classification

#### 2.2.1. Solubility

In order to determine the dose number (Do), solubility measurements were carried out at reference pHs 1.2, 4.5 and 6.8; pH 7.5 was also studied for better understanding of the release profiles. Saturated solutions were prepared by adding excess amounts of drug to these media and shaking on a shaker bath for 24 h under constant vibration. During the test the presence of undissolved solid was checked to ensure that the solution could reach saturation. Samples were taken at pre-determined times up to 24 h, centrifuged and the supernatant was analyzed by high performance liquid chromatography (HPLC).

Determination of CPT was carried out at 25 °C on a stainless steel column Waters model Nova Pak C-18 150 mm length, 3.9 mm in diameter and particle size of 4 µm preceded by a Teknocrroma TCR-C130-B precolumn. The solvent delivery system (Alliance System (Waters 2695)) was used to deliver a mobile phase 70:30 trifluoroacetic acid aqueous solution at pH 3 and acetonitrile. The flow rate was 1 mL/min. Detection was performed using a fluorescence detector (Waters 2475) with an excitation wavelength of 363 nm and an emission wavelength of 550 nm.

#### 2.2.2. Permeability

**2.2.2.1. *In vitro* permeability studies in Caco-2.** Caco-2 cells were grown in Dubelcco's Modified Eagle's Media containing l-glutamine, fetal bovine serum and penicillin–streptomycin. Cell monolayers were prepared by seeding 250,000 cells/cm<sup>2</sup> on the polycarbonate insert placed inside the wells. They were maintained at 37 °C temperature, 90% humidity and 5% CO<sub>2</sub> for 4 days until confluence and 21 days after seeding to make sure that all transporters were expressed. Afterwards, the integrity of each cell monolayer was evaluated by measuring the *trans*-epithelial electrical resistance (TEER). Hank's balanced salt solution (HBSS) supplemented with HEPES was used to fill the receiver chamber and to prepare the drug solution that was placed in the donor chamber. Drug transport studies were performed from apical-to-basal (A-to-B) direction using the concentrations of 5 µM, 10 µM, 50 µM. The permeability of metoprolol (100 µM) was also determined in order to compare the results, due to the permeability value of this compound is used as reference in BCS classification.

Transport studies were conducted in an orbital shaker at constant temperature (37 °C) and agitation rate (50 rpm). Four samples were taken from the receiver side at prefixed sample times 15, 30, 45 and 90 min. Samples of the donor side were taken at the beginning and at the end of the experiment. The amount of compound in cell membranes and inside the cells was determined at the end of experiments in order to check the mass balance and the percentage of compound retained in the cell compartment as always less than 5% [27].

The apparent permeability coefficient was calculated according to the following equation:

$$C_{\text{receiver},t} = \frac{Q_{\text{total}}}{V_{\text{receiver}} + V_{\text{donor}}} + \left( (C_{\text{receiver},t-1} \cdot f) - \frac{Q_{\text{total}}}{V_{\text{receiver}} + V_{\text{donor}}} \right) \cdot e^{-P_{\text{eff},0,1} \cdot S \cdot \left( \frac{1}{V_{\text{receiver}}} + \frac{1}{V_{\text{donor}}} \right) \cdot \Delta t}$$

where  $C_{\text{receiver},t}$  is the drug concentration in the receiver chamber at time  $t$ ,  $Q_{\text{total}}$  is the total amount of drug in both chambers,  $V_{\text{receiver}}$  and  $V_{\text{donor}}$  are the volumes of each chamber,  $C_{\text{receiver},t-1}$  is the drug concentration in receiver chamber at previous time,  $f$  is the sample replacement dilution factor,  $S$  is the surface area of the monolayer,  $\Delta t$  is the time interval and  $P_{\text{eff}}$  is the permeability coefficient which might be  $P_{\text{eff}0}$  or  $P_{\text{eff}1}$ .

The permeability is calculated taking into account the accumulated amounts of the drug in acceptor chamber at several times and the

simultaneous consideration of the concentration change in the donor chamber. For calculating permeability values linear or nonlinear regression models can be used, depending of the assumption about sink conditions on the receptor side and about the concentration change on donor side. The “classical” linear model requires sink conditions maintenance in acceptor as well as a nearly constant concentration in donor. As Mangas-Sanjuan et al. demonstrated Non-Sink modified method is a precise and accurate equation for calculating the permeability in sink and non-sink conditions and with or without change in donor concentrations [28]. Linear regression models (Sink and Sink Corrected), are not valid under non-sink conditions and even under sink conditions but the system variability is high. In general, when the “classical equation” (i.e linear model) is applied when sink conditions are not present, the calculated permeability value is biased.

The non-linear regression to fit the equation to data was performed in Excel® using Solver tool for minimization of the sum of squared residuals.

**2.2.2.2. Small intestine and large intestine in situ perfusion technique.** The animal study was approved by the Scientific Committee of the Faculty of Pharmacy (project reference A1330354541263) and followed the guidelines described in the EC Directive 86/609, the Council of the Europe Convention ETS 123 and Spanish national laws governing the use of animals in research (Real Decreto 223/1988, BOE 67, 18-3-98:8509-8511).

The absorption rate coefficient ( $k_a$ ) and permeability values ( $P_{app}$ ) of CPT were determined in two segments of gastrointestinal tract: entire small intestine and colon. Test solutions were prepared freshly before use. Three concentrations of CPT (5  $\mu$ M, 10  $\mu$ M, 50  $\mu$ M) and four rats per group ( $n = 4$ ) were tested. The permeability of metoprolol (100  $\mu$ M) was also studied as a benchmark, since it determines whether a drug is high or low permeability [29]. *In situ* perfusion of the whole small intestine (“closed loop”- Doluisio’s Technique) [30] adapted as described by Ferrando et al. [31] was used to characterize the absorption rate coefficient and the permeability value of CPT. Male Wistar rats, four hours fasted with free access to water, were anesthetized using a mixture of diazepam (Valium, Roche) (1.67 mg/kg), ketamine (Ketolar; Parke-Davis) (50 mg/kg) and atropine (Atropine sulphate; Braun) (1 mg/kg) and placed on heated surface to be maintained at 37 °C. A midline abdominal incision was made. The intestinal segment was manipulated carefully to minimize any intestinal blood supply disturbances. In order to prevent enterohepatic recycling and the presence of bile salts in lumen, the bile duct was closed before the perfusion.

Briefly, the method consists of creating a compartment in the small intestine with the aid of two syringes and two three-way stopcock valves. After cleaning and conditioning the intestine segment with a physiologic solution (isotonic saline adjusted to pH 7.0 with 1% Sørensen phosphate buffer (v/v), 37 °C), the drug solution (10 mL) is placed in the intestinal segment.

The absorption rate coefficient and the permeability value in the colon were evaluated with a similar technique to that used for the whole small intestine. The colon is placed from the end of cecum sac to rectum. The drug solution (5 mL) was introduced in the isolated compartment.

Sampling of the perfusion in both isolated segments was carried out at fixed times, after 5 min at intervals of 5 min up to 30 min [32,33]. In order to separate solid components (mucus, intestinal contents) from the samples, they were centrifuged 5 min at 5000 r.p.m. All samples were analyzed immediately by HPLC.

The reduction in the volume of the perfused solutions at the end of the experiments was significant (up to 20%), and a correction became necessary in order to calculate the absorption rate constants accurately. Water reabsorption was characterized as an apparent zero order process. A method based on direct measurement of the remaining volume of the test solution was employed to calculate the water reabsorption

zero order constant ( $k_o$ ). The volume at the beginning of the experiment ( $V_0$ ) was determined on groups of three animals, while the volume at the end ( $V_t$ ) was measured on every animal used. The concentration in the samples was corrected as

$$C_t = C_e(V_t/V_0)$$

where  $C_t$  represents the concentration in the gut that would exist in the absence of the water reabsorption process at time  $t$  and  $C_e$  the experimental value. The  $C_t$  values (corrected concentrations) were used to calculate the actual absorption rate coefficient [34]. The absorption rate coefficients ( $k_a$ ) of compounds were determined by nonlinear regression analysis of the remaining concentrations in lumen  $C_t$  versus time.

$$C_t = C_0 \cdot e^{-k_a t}$$

These absorption rate coefficients were then transformed into permeability values using the relationship:  $P_{app} = k_a R/2$ , where  $R$  is the effective radius of the intestinal segment, calculated from the area/volume relationship: 10 mL perfusion volume and an intestinal length of 100 cm for the whole small intestine, and 5 mL perfusion volume and a length of 10 cm for the colon.

The permeability values obtained for the different concentrations of CPT and metoprolol were evaluated using the ANOVA statistical test for independent samples with a 95% confidence level. For the post-hoc analysis, a parametric or non-parametric test was selected based on the homogeneity of the variances determined by the Levene test.

### 2.3. Hydrogel formation and characterization

#### 2.3.1. Hydrogel preparation

It was first prepared a solution of chitosan by weighting 2 g (6 mmol) of polymer in 100 mL of acetic acid 87 mM. Then CPT (1.4  $\mu$ mol) previously solubilized in NMP (2.87 mM) was incorporated and finally different amounts of THPC (0.03, 0.05, 0.1, 0.2 mmol) were added in order to obtain a degree of substitution (moles of THPC/moles of chitosan repetitive units) of 24%, 40%, 80% and 160%, respectively. The gelation occurred within 5–10 s of stirring at room temperature. Hydrogels were washed to eliminate drug entrapped in the surface layer to avoid a burst effect at the drug release study, and finally they were lyophilized.

To characterize *in vivo* mucoadhesiveness the hydrogel was fluorescently marked. For this proposal, chitosan (1 mg/mL) was added to a basic aqueous solution of rhodamine B isothiocyanate (2 mM). The reaction was kept under vigorous stirring, afterwards it was filtered, washed with water / methanol and water/ethanol and the final product was lyophilized.

The nomenclature of the various hydrogel compositions prepared according to the described methodology is shown in Table 1.

#### 2.3.2. Hydrogels characterization

**2.3.2.1. Elementary analysis.** The determination of the carbon,

**Table 1**  
Hydrogels scheme based on their composition.

	Chitosan	Crosslinking percentage (THPC/chitosan)			
		24%	40%	80%	160%
Hydrogels	LMW	L24	L40	L80	L160
	MMW	M24	M40	M80	M160
	HMW	H24	H40	H80	H160
Hydrogels with CPT/ NMP	LMW	L24-CPT	L40-CPT	L80-CPT	L160-CPT
	MMW	M24-CPT	M40-CPT	M80-CPT	M160-CPT
	HMW	H24-CPT	H40-CPT	H80-CPT	H160-CPT
Hydrogels with rhodamine	LMW				RL160
	MMW				RM160
	HMW				RH160

hydrogen and nitrogen content of the solid state samples was carried out on a LECO CHNS-932 equipment using sulfanamide as reference.

**2.3.2.2. Thermogravimetric analysis.** Thermogravimetric analysis was performed on a previously calibrated Perkin-Elmer Diamond electrobalance with platinum as a reference material (Pt/Rh (10%)). Powder samples placed into platinum sample holders were heated in air or argon flow (100 mL/min) from room temperature to 900 °C at a heating rate of 10 °C/min. Before measuring the samples, the baseline was measured on an empty sample holder to correct the results obtained for the formulations.

**2.3.2.3. X-ray diffraction.** Pulverized samples were placed and pressed into a sample holder to obtain a flat and uniform surface. X-ray diffraction diagrams were recorded using a Philips X'Pert Plus diffractometer with CuK $\alpha$  radiation ( $\lambda = 1.5406 \text{ \AA}$ , 40 kV), sweep velocity in the range of 0.6° to 10.0° (2 $\theta$ ) per minute, with a step of 0.02° (2 $\theta$ ) and an analysis time of 5 s.

**2.3.2.4. Inductively coupled plasma mass spectrometry (ICP-MS).** The phosphorus content was determined by dissolving the compound in 3–10 mL of HNO<sub>3</sub>/HCl, diluting with bidistilled water up to 30–50 mL and measuring the solution on a Varian 715-ES inductively coupled plasma mass spectrometer.

**2.3.2.5. Scanning electron microscopy.** To observe the cross sections of the chitosan hydrogels the samples were adhered with a double-binder adhesive tape on cylindrical sample holders. Samples were coated with an Au/Pd layer using a Polaron sputter-coat model SC7640 at a vacuum pressure of 0.6 mbar and at 0.8 mA for 120 s. Images were taken with a scanning microscope Hitachi model S4800 with an acceleration voltage of 5 Kv and a working distance of 8 mm.

**2.3.2.6. Swelling.** The swelling studies were carried out twice to determine the influence of several factors, as MW of chitosan, ratio of crosslinking and media pH.

The first assay studied the influence of the degree of crosslinking and the MW of chitosan. The test was carried out at pH 7.5 at 37 °C during 48 h (time enough to reach swelling equilibrium). At the end of the assay, hydrogels were withdrawn from the solutions, blotted with a filter paper to remove surface absorbed water and weighted.

The second assay studied the influence of pH and MW of chitosan in the swelling characteristics of the hydrogels. The study was carried out in different media pH (pH 1.2, pH 4.5, pH 6.8 and pH 7.5) at 37 °C. Hydrogels were assayed for 48 h. At determined times the hydrogels were withdrawn from the solutions, blotted with a filter paper, weighted and placed again within the media. For both experiments it was confirmed that after a 48 h period the hydrogels had reached their equilibrium of swelling. The weight uptake of the hydrogels is expressed by the following equation:

$$S = [(W_s - W_d)/W_d]$$

where  $S$  is the swelling result of the hydrogel and  $W_d$  and  $W_s$  are the weights of the samples in the dry and swollen states, respectively. Each swelling experiment was carried out in triplicate and the average values are reported.

**2.3.2.7. Toxicity.** The ability of the hydrogels to interfere with the growth of Caco-2 cells was determined *in vitro* using the 3-(4,5-dimethylthiazol-2-yl)-2,5-diphenyltetrazolium bromide (MTT) assay based on the metabolic reduction reaction in mitochondria of the yellow-colored compound 3-(4,5-dimethylthiazol-2-yl)-2,5-diphenyltetrazole (MTT) into the blue-colored formazan. The formation of the blue compound can be followed spectrophotometrically at 490 nm and the absorbance value is proportional to the number of living cells.

Assays were carried out in 96-well microliter plates with flat-bottomed wells seeding 25,000 cells per well. Cultures were grown at standard conditions of humidity, CO<sub>2</sub> concentration and temperature. 24 h after seeding the medium was replaced with a fresh medium and 50  $\mu$ L of the dispersed gel samples (5 mg/mL in PBS) were added. Plates were incubated for 24, 48, or 72 h and then, in order to evaluate the percentage of cell survival, 20  $\mu$ L of MTT solution (5 mg/mL) were added to each well. The samples were incubated at 37 °C for 3 h to allow reaction for the formazan formation. The content of each well was removed and the dark blue crystals were redissolved in DMSO. Absorbance was measured at 490 nm with a Labsystems Multiskan EX plate reader. Assays were carried out in quadruplicate for each treatment. Toxicity values of untreated wells and treated with similar chitosan hydrogels but with glutaraldehyde as crosslinker has been used to compare. Cell survival data were expressed as a percentage of the absorbance of the untreated control.

**2.3.2.8. Biocompatibility.** The viability of Caco-2 cells after growing on the hydrogel was analyzed with the aid of staining kit LIVE/DEAD®. For assays, hydrogels were obtained and culture medium was added and replaced several times during 24 h in order to hydrogels were saturated in culture medium. 24 h later Caco-2 cells were seeded. Several days later, the staining procedure was performed using de LIVE/DEAD® viability/toxicity kit for mammalian cells that provides a two-color fluorescence cell viability assay using calcein AM and ethidium homodimer based on the intracellular esterase activity and plasma membrane integrity. Polyanionic dye calcein is well retained within live cells where takes place the enzymatic conversion to fluorescent calcein producing green fluorescence in live cells (ex/em 495 nm/515 nm). Ethidium homodimer is excluded by the intact plasma membrane of live cells but can stain the damaged or dead cells producing red fluorescence in presence of DNA (ex/em 528 nm/617 nm). After the staining procedure cells were visualized with the aid of epifluorescence microscopy (Nikon Eclipse E800). Samples of live cells were used as control of green fluorescence. Dead cells were used as control of red fluorescence.

The differences between the values of cellular survival were studied by the statistical ANOVA test with a level of significance  $\alpha = 0.05$ . As post-hoc test, parametric or non-parametric tests were selected based on the homogeneity of the variances determined by the Levene test.

## 2.4. Mucoadhesiveness

### 2.4.1. *In vitro* mucoadhesiveness test

As *in vitro* approach to determine the mucoadhesiveness of hydrogels at the gastrointestinal tissues the following study was carried out. Wistar rats (12 weeks old) were sacrificed by intraperitoneal administration of 60 mg/kg of pentobarbital sodium and their gastrointestinal tissues (stomach, duodenum, jejunum, ileum and colon) were excised. Each tissue was slowly washed with 0.9% NaCl saline solution and was opened to expose the lumen.

The tissue was placed on a 45° inclined surface with a continuous buffer circulation of 4 mL/min. The lyophilized hydrogels (L160, M160, H160) were hydrated for 45 min in pH 1.2 and then placed on the stomach tissue. After 1.5 h flowing the pH 1.2 buffer on the stomach, hydrogels were moved to the duodenal tissue and a buffer at pH 4.5 was pumped for 15 min. The same procedure was carried out to study the mucoadhesiveness on ileum and jejunum, using a pH 6.8 buffer for 1.4 h on each segment. Finally the remaining sample of gel was placed on the colon and kept under the pH 7.5 buffer up to 48 h.

### 2.4.2. *In vivo* mucoadhesiveness test

The *in vivo* mucoadhesiveness assays adhered to the ethical practices and the protocol was approved by the ethical committee (2015/VSC/PEA/00008).

In order to evaluate the gastrointestinal transit of the hydrogel

formulations Wistar rats weighing 230–250 g were used. Animals were fasted for 2–4 h before experiments and during the experiment, with water *ad libitum*. Rhodamine-labeled hydrogels were introduced into capsules and administered orally by gavage. Barium sulphate was used as a control of intestinal transit. At certain times (1, 2 and 4.5 h) animals were sacrificed, the gastrointestinal tract was taken out and fluorescence and radio-opacity signal were studied at the In-Vivo FX Pro system.

Fluorescence images of rhodamine-labeled hydrogels were superposed with photographs of the tracts using ImageJ®. With this software the lengths of the gastrointestinal tracts and the location of the hydrogels and barium sulfate were measured for each animal. Calculations of the relative location of formulations and controls against total length of the gastrointestinal tract were performed using an Excel spreadsheet.

For this procedure 4 groups of 9 animals each one were used: group 1 received formulation RL160, group 2, formulation RM160; group 3, formulation RH160 and group 4 received barium sulphate as a control. Three animals of each group were sacrificed at each prefixed time.

#### 2.4.3. In vitro drug release

In vitro drug release studies were performed in 200 mL of dissolution medium, which was placed in an air shaker bath adjusted to 100 rpm/min and maintained at 37 °C. At specific time intervals, aliquots of samples were withdrawn and replaced with an equal amount of fresh dissolution media. The amount of remaining CPT at the end of the test was quantified by degrading the hydrogel with HCl 35%. Drug content in each sample was immediately determined by HPLC.

Hydrogels were assayed during 48 h, the pH of the medium was increased at certain times to simulate gastrointestinal conditions. The schedule was summarized in Table 2.

Hydrogels with different MW of chitosan and different degree of crosslinking were assayed to obtain their drug release profiles. Each experiment was carried out in triplicate and the average values are reported. Data fitting to Korsmeyer-Peppas [35] model was performed to establish the kinetic model of drug release from the hydrogels. Experimental values were used up to a release percentage of 60% of the total amount present in the hydrogel.

### 3. Results

#### 3.1. Camptothecin biopharmaceutical classification

Solubility and permeability studies of this drug have been performed in order to classify it according to BCS.

##### 3.1.1. Solubility

The solubility as well as dose number values are shown in Table 3. Dose number (Do) is the ratio of drug concentration in the administered

**Table 2**  
Schedule of the *in vitro* release test.

Time (h)	pH	Simulated tract area	Composition
1.5	1.2	Stomach	78 mL HCl 0.1 N pH 1.2
0.25	4.5	Duodenum	78 mL HCl 0.1 N (pH 1.2) + 112 mL phosphate buffer pH 7.5 (50 mM) + 2.6 mL NaOH 1 M
2.75	6.8	Jejunum, ileum	78 mL HCl 0.1 N (pH 1.2) + 112 mL phosphate buffer pH 7.5 (50 mM) + 5.2 mL NaOH 1 M
Until 48	7.5	Colon	78 mL HCl 0.1 N (pH 1.2) + 112 mL phosphate buffer pH 7.5 (50 mM) + 6.9 mL NaOH 1 M

**Table 3**  
Solubility and dose number of CPT at different pH values.

Media pH	Solubility (µg/mL)	Do
pH 1.2	14.21	3.1
pH 4.5	6.42	6.8
pH 6.8	14.71	3.0
pH 7.5	9.35	4.7

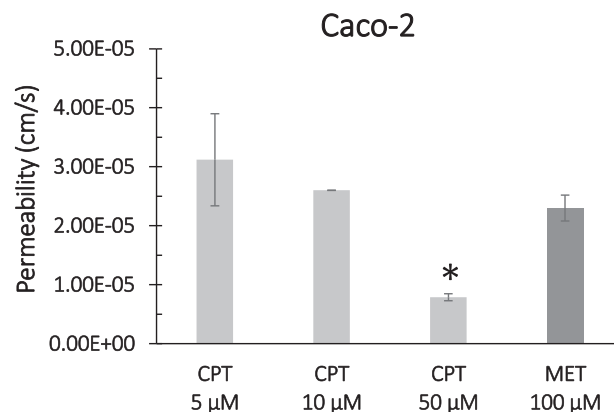


**Fig. 1.** Permeability (cm/s) of metoprolol and different concentrations of CPT (5 µM, 10 µM and 50 µM) in Caco-2 cells 21 days postseeding. (\*) Denotes statistical differences of CPT 50 µM with CPT 5 µM, CPT 10 µM and metoprolol.

volume (250 mL) to the solubility of the drug in water, which may also be viewed as the number of glasses of water required to dissolve the drug dose. A dose number equal or lower than 1 ( $Do \leq 1$ ) indicated high-solubility, and Do greater than 1 signified a low-solubility compound [36]. The solubility of CPT in aqueous solutions is in the range of 6–14 µg/mL depending on the pH value of the medium.

##### 3.1.2. Permeability

Permeability values of CPT and metoprolol in Caco-2 cells after 21 days post-seeding are shown in Fig. 1. As shown in the graph, the permeability of CPT 50 µM is significantly lower than that of metoprolol. Likewise, there are statistically significant differences for CPT permeabilities between 5 and 50 µM and between 10 and 50 µM.

Permeability of CPT (Fig. 2) in small intestine at low concentrations of CPT (5 and 10 µM) is higher than that of the reference drug, metoprolol. However, the permeability of CPT decreases significantly at higher concentrations (50 µM), being lower than that of metoprolol. In contrast, in the colon, CPT (at any concentration tested), has significantly lower permeability than metoprolol. The results obtained *in situ* agree with those observed in the study of permeability in Caco-2.

#### 3.2. Hydrogels characterization

##### 3.2.1. Thermogravimetric analysis

For the first stage of thermogravimetric analysis of chitosan and chitosan crosslinked with THPC there is a weight loss up to 100 °C due to adsorbed water elimination. Next stages correspond to the thermal decomposition and pyrolysis which show differences between the polymer and the hydrogel. Chitosan decomposition is observed at 300 °C; in contrast, the temperature of maximum decomposition of hydrogels occurs between 200 °C and 300 °C depending on the degree of crosslinking. The greater the crosslinking of the polymer the lower the decomposition temperature is. In addition, at temperatures above 600 °C the TGA graphic shows a residue in the hydrogels (10–25%), being negligible in the case of uncrosslinked polymer. The same results are observed for any molecular weight of crosslinked chitosan studied. It has been found that the labeling of the polymer with rhodamine do

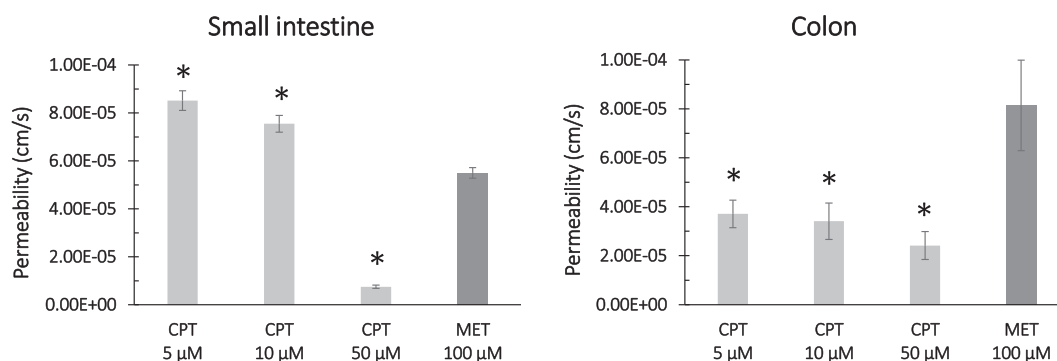


Fig. 2. Permeability (cm/s) of metoprolol and CPT at different concentrations in the small intestine and colon. (\*) Shows significant statistical differences between metoprolol (100 μM) and CPT (5 μM, 10 μM and 50 μM).

not affect the thermal stability of the samples.

Considering the temperature at which the maximum thermal degradation occurs as an indicator of the thermal stability, the thermal stability decreases as the crosslinking degree increases: Chitosan > Chitosan-THPC 24% > Chitosan-THPC 40% > Chitosan-THPC 80% > Chitosan-THPC 160%.

### 3.2.2. X-ray diffraction

According to X ray diffraction studies, the crosslinked chitosan is more amorphous than the starting polymer. Chitosan presents two diffraction peaks at  $2\theta = 10^\circ$  and  $20^\circ$ . A 24% of chitosan-THPC crosslinking decreases polymer crystallinity, since there is no peak at  $20^\circ$ . A higher incorporation of crosslinking agent (160%), increases the amorphization of the polymer, evidenced by the absence of both peaks of the diffractogram. Also, it is observed that the encapsulation of the drug does not modify the amorphized polymer in the presence of the crosslinking agent.

The crosslinking process affects the thermal stability of chitosan membranes as well as their supramolecular structure. Molecular weight of chitosan do not influence the stability properties of chitosan.

### 3.2.3. Elementary analysis

Percentages of carbon, nitrogen and hydrogen in hydrogels are slightly lower than the corresponding in naive chitosan. The ratio of carbon, nitrogen and hydrogen decreases as the degree of crosslinking of the polymer increases. Results are similar for any molecular weight of chitosan studied. In conclusion, the addition of crosslinker is effective in every single chitosan.

### 3.2.4. Inductively coupled plasma mass spectrometry (ICP-MS)

ICP-MS results of the crosslinked polymer with different percentages of THPC shows that the higher the percentage of crosslinker added, the higher the percentage of phosphorus incorporated into the organic network. Also, the phosphorylation process is found to be very similar in percentage between polymers of different molecular weight with the same crosslinking percentage.

### 3.2.5. Scanning electron microscopy

SEM images (Fig. 3) show the internal structure of the lyophilized hydrogel. No evident differences were observed between the hydrogels formed by chitosan of different molecular weights. The structure of the polymer network in all cases is composed of interconnected irregularly sized cavities and pores.

### 3.2.6. Swelling

The swelling studies have been carried out in two parts to assess the influence of several factors: polymer MW, percentage of crosslinking agent and pH of the medium.

In the first study, the swelling equilibrium of the hydrogels with

different percentage of crosslinking and different MW of the polymer at pH 7.5 was determined. Results are outlined in Fig. 4.

In the second test, the swelling profiles of hydrogels of different MW with a crosslinking percentage of 40% were obtained and the influence of pH and MW on the swelling dynamics was evaluated. For simplicity, only swelling values corresponding to 48 h are represented in Fig. 5. The results show the pH dependence in the swelling of the hydrogel, since at pH 1.2 the swelling is significantly greater than in the other media.

### 3.2.7. Toxicity

The toxicity of the hydrogels has been assessed by determining the percentage of cell survival after exposure of Caco-2 cultures to hydrogels with different percentage of crosslinking (M24, M40 and M80). Fig. 6 shows the cell survival after 24, 48 and 72 h of exposure compared to a negative control, absence of exposition, and to similar hydrogels but containing glutaraldehyde as linking agent as positive control (G24, G40 and G80). Data are expressed as a percentage of the absorbance of the untreated control.

M24 hydrogel did not show toxicity at any exposure time. Application of M80 for 24 and 72 h resulted in a percentage of cell survival around 90%. The homologous hydrogel prepared using glutaraldehyde as linker, applied during the same time, provided values of 8% of cell survival. Results obtained for all the glutaraldehyde hydrogels indicate the advantage to use THPC as a linker agent.

Long-term cell culture results (one month) have shown that proliferation of cells exposed to hydrogels is comparable to controls, confirming the low toxicity nature of hydrogels (data not shown).

### 3.2.8. Cytocompatibility

The ability of hydrogels to allow the growth of Caco-2 cells on their surface has been evaluated by staining with the LIVE/DEAD cytotoxicity/viability kit and microscopy visualization with phase contrast and fluorescence (Fig. 7). Living cells stained with AM calcein and dead cells stained with ethidium homodimer-1 were observed using green and red filters, respectively. As can be seen in Fig. 7 most cells are still alive after 3 and 7 days of their seeding, which demonstrates the cytocompatibility of hydrogels.

### 3.2.9. Mucoadhesiveness

**3.2.9.1. In vitro mucoadhesiveness.** Mucoadhesive properties have been evaluated *in vitro* using gastric and intestinal (duodenum, jejunum, ileum and colon) rat tissues. The negative control slides off the assembly during the first five minutes. On the contrary, all hydrogels tested remained adhered, to at all tissues and pH conditions, without displacement due to gravity or the flow drag during all the study.

**3.2.9.2. In vivo transit time.** In order to confirm the adhesive behaviour observed in the *in vitro* assay and to evaluate the gastrointestinal transit

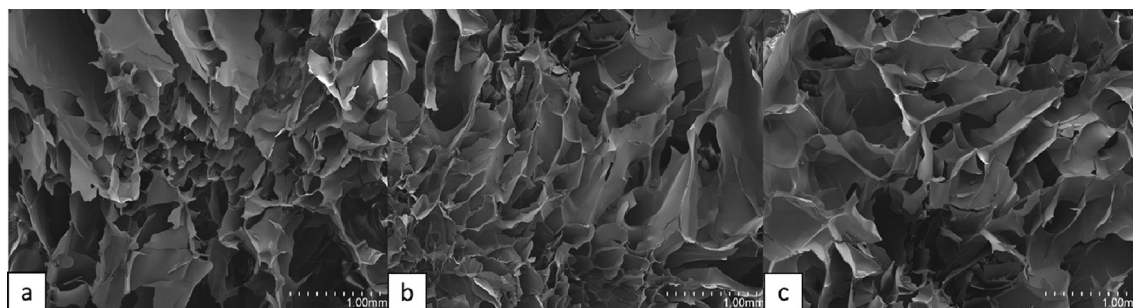


Fig. 3. Scanning electron microphotographs of hydrogels of (a) low MW chitosan, (b) medium MW chitosan, (c) high MW chitosan, crosslinked with THPC 160%.

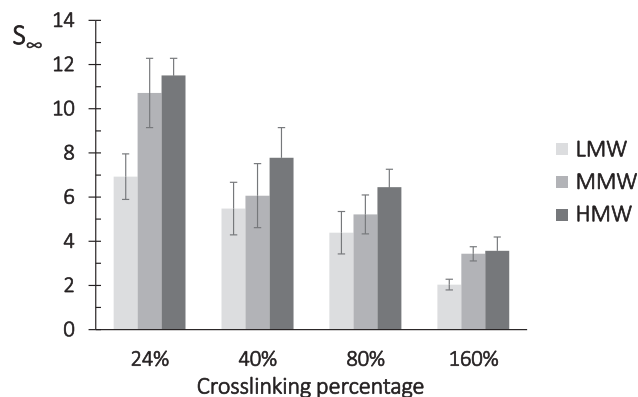


Fig. 4. Swelling values in equilibrium,  $S_{\infty}$ , after 48 h at pH 7.5. Hydrogels are referred to the MW of chitosan (LMW: low molecular weight, MMW: medium molecular weight, HMW: high molecular weight) and the percentage of cross-linking.

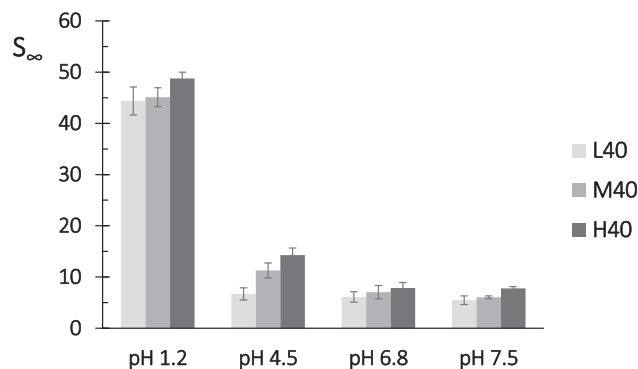


Fig. 5. Graphical representation of swelling values of hydrogels crosslinked at 40% at different pH of exposure.

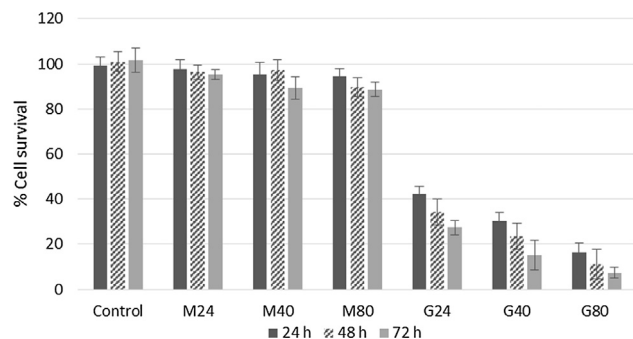


Fig. 6. Percentages of Caco-2 cells survival in absence (control) and presence of hydrogels M24, M40, M80, G24, G40 and G80 at 24, 48 and 72 h. (\*) = Statistically significant differences with the corresponding control.

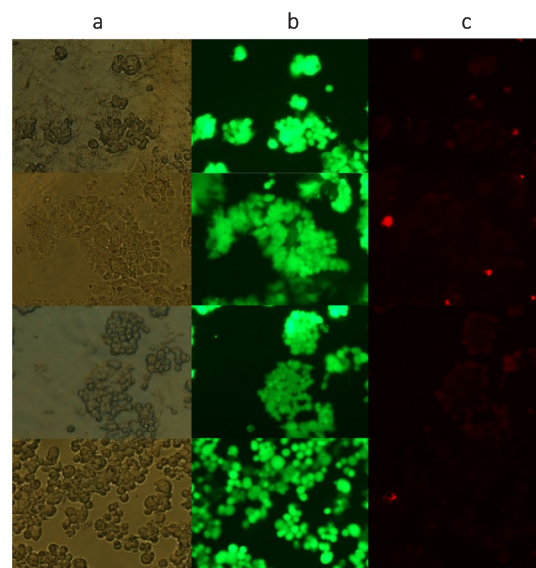


Fig. 7. Microscopy images obtained after staining of Caco-2 cells grown on hydrogels: (a) image taken with phase contrast, (b) image of living cells taken with fluorescence (green filter), (c) image of dead cells taken with fluorescence (red filter). (For interpretation of the references to colour in this figure legend, the reader is referred to the web version of this article.)

of different hydrogels, formulations labelled with rhodamine and controls of barium sulphate were administered orally to Wistar rats. The evolution of the hydrogels was monitored during 4.5 h by taking fluorescence and radiographic images at different times (1, 2 and 4.5 h). Photos and fluorescent images of each gastrointestinal tract have been overlapped to better locate the formulation and to show representative images of hydrogel evolution (Fig. 8).

As can be seen in Fig. 9, the barium sulphate seems to progress more compactly along the gastrointestinal tract, in contrast to test formulations, which remain retained in said tract. Small intestine (duodenum, jejunum, ileum) represent the  $81 \pm 2.5\%$  of whole intestine length, and large intestine the other  $19 \pm 2.5\%$ . One hour after administration, there are no differences between tested formulations and control. After two hours, barium sulphate has progressed faster; in contrast, hydrogels location is more extensive due to the different progression of the formulation (some parts are retained due to the adhesion and others ones move faster). At 4.5 h after administration, the progression of the control is between 80 and 90% of the intestine, while the formulations have been retained between 30 and 70% of the intestine length. No differences were observed between different MW of the polymer.

### 3.2.10. In vitro drug release

The release studies have been performed in a medium with variation of pH at different times to simulate as much as possible the physiological conditions. The pH changes occurred immediately after sampling

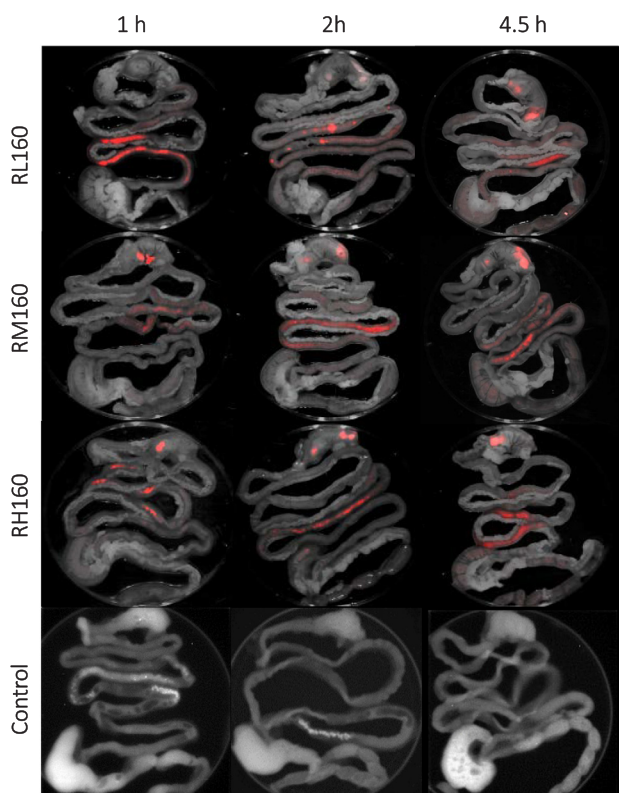


Fig. 8. Fluorescence images of RL160, RM160, RH160 formulations and X-ray images of barium sulphate after 1 h, 2 h and 4.5 h of oral administration.

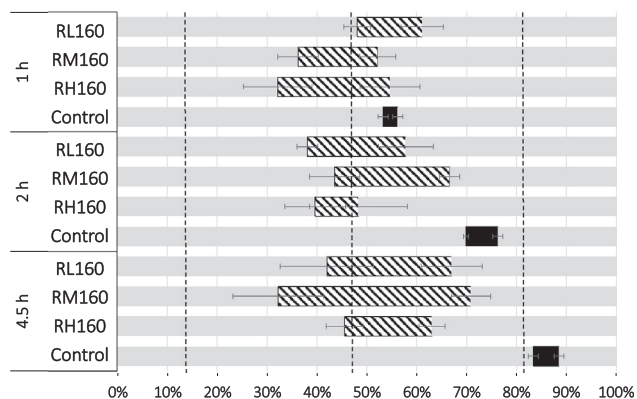


Fig. 9. Representation of the progression of hydrogels (striped bars) and barium sulphate (black bars) with respect to the length of the whole intestine (black bars). The dotted lines delimit the intestinal sections: duodenum, jejunum, ileum and large intestine.

at the times: 90, 105 and 270 min (1.5, 1.75 and 4.5 h) (Fig. 10).

From the results obtained it is concluded that approximately 30% of the drug contained in the hydrogel is released after 1.5 h at pH 1.2, leaving a remaining 70% susceptible of release throughout the intestine. At 48 h, the hydrogels have released between 65 and 97%, depending on the composition of the hydrogel.

According to data fitting to Korsmeyer-Peppas model, the kinetic constant values range from 0.22 to 0.33 h<sup>-1</sup> and the diffusional exponent is, in all cases, less than 0.45. This indicates that drug release occurs by diffusion through the pores and the swollen matrix. There are differences in the release profiles of hydrogels formed by low and high molecular weight chitosan.

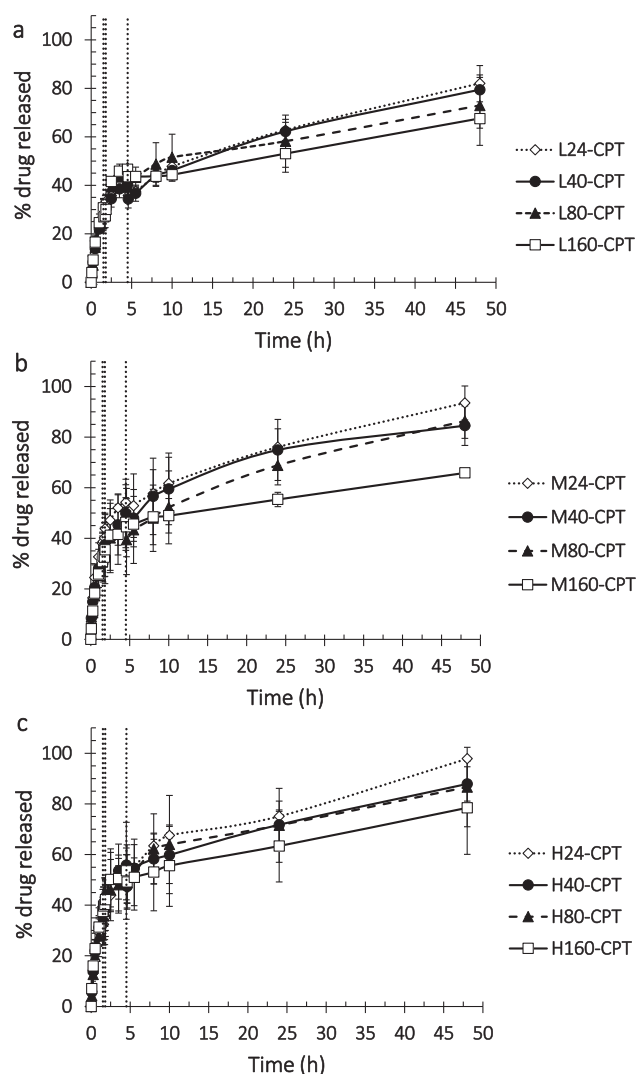


Fig. 10. In vitro release studies profiles simulating physiological conditions.

#### 4. Discussion

Regarding the biopharmaceutical classification of CPT, the solubility of the drug in aqueous solutions is in the range of 6–14 µg/mL depending on the pH value of the medium. According to published studies, the human dose is 6 mg/m<sup>2</sup>/day [37]. For this CPT dose, the values of Do are higher than 1 in all cases, indicating that it is a drug of low solubility.

CPT delivery from a formulation is expected to take place along all intestine. For this reason, as well as to confirm the results obtained *in vitro*, the permeability in both intestinal segments, small and long, was evaluated through *in situ* permeability studies. The method proposed by Doluisio was selected to perform the studies because it has several advantages over other similar ones, since it is carried out without recirculation, which avoids the disorganization of the aqueous diffusion layer adjacent to the membrane and the alteration of the physiological conditions. In addition, conditions of blood flow and tissue integrity are similar to those existing *in vivo*. Moreover, this methodology has been previously compared with single pass perfusion and validated to have the same predictability of human permeability [34,38–40].

According to our results and those published by other authors it is deduced that the CPT is absorbed by both passive diffusion and active transporters [12]. At high concentrations, at which the transporters are saturated and mainly passive diffusion takes place, CPT permeability is low; whereas at low concentrations, at which the functionality of

absorption transporters can be observed (mainly in the small intestine and Caco-2 at 21 days) an increase of the permeability of this drug is observed. When the CPT concentration is equal to or greater than 50  $\mu\text{M}$ , the absorption transporters become saturated, so the drug permeability is reduced.

Therefore, CPT can be considered a drug of high permeability in the small intestine for concentrations  $\leq 10 \mu\text{M}$  and of low permeability for concentrations  $\geq 50 \mu\text{M}$ . These differences in permeability as a function of concentration can be attributed to the existence of active absorption and secretion components as proposed in some studies [11,12]. In contrast, this drug presents low permeability in colon due to the lack of transporters in this intestinal segment.

Based on the results obtained in the solubility and permeability studies, it is concluded that CPT is a drug of low solubility and its permeability depends on the concentration and intestinal segment in which it is absorbed. Therefore, it can be classified as a class II drug at low concentrations ( $\leq 10 \mu\text{M}$ ) in the small intestine and a class IV drug at high concentrations ( $\geq 50 \mu\text{M}$ ) in the small intestine and at any concentration in the large intestine.

In this study it has been shown that CPT is a good candidate to be administered within an oral controlled release system, since this system would provide low concentrations of drug in the intestinal lumen that could be absorbed quickly. This would increase drug efficacy and would reduce its toxicity, since the residence time in the intestinal lumen outside the delivery system would be reduced. There are some research studies that vectorize camptothecin to colon in order to treat colorectal cancer but it is interesting too to design systems that allow and promote the absorption of camptothecin using its pharmacokinetics characteristics.

Release studies have demonstrated that this polymeric system exhibits a modified release of the drug capable of delivering the drug for at least 48 h. The release profiles can be adjusted to Korsmeyer-Peppas mathematical model, indicating that drug release occurs by diffusion through the swollen matrix and through the pores. Our results show that changing crosslinker and camptothecin concentrations it is possible to get a variety of release profiles. Moreover, this system overcome the limitation of other poor loading systems published [41].

Swelling studies show the pH dependence in the swelling of the hydrogel, since at pH 1.2 the swelling is significantly greater than in the other media. This is due to the protonation of the chitosan amino groups which increases the electrostatic repulsion between the chains and favours the expansion of the chains. The swelling at pH 6.8–7.5 is minimal, while at pH 4.5 it is slightly higher but much lower than at pH 1.2. The explanation for this result is the same, since at pH 4.5 the amino groups of chitosan are protonated but at a lower proportion than at pH 1.2 (lower degree of ionization of the polymer implies less electrostatic repulsion). In general, the higher the chitosan MW and the lower the degree of crosslinking, the greater the swelling of the hydrogel is.

The mathematical model that better fits experimental data is order two kinetic model, described by Schott for the swelling of crosslinked semicrystalline polymers, such as cellulose and gelatin [42]. This author explains that the rate of swelling can be considered directly proportional to the percentage of the swelling capacity still available at a given time and to the total internal specific boundary area enclosing those sites capable of swelling that have not yet become hydrated and swollen at that time. Toxicity studies concluded that the hydrogels have low toxicity compared with other hydrogels obtained with aldehydic linkers as the reduction of survival is in the range of 10 to 20% and cytocompatibility studies demonstrate that hydrogels allow cell growth over their surface. Our results are consistent with those obtained by Chung et al. [21] that reported alive cells encapsulation using a protein-based hydrogels crosslinked with THPC. Despite other linkers as genipin or spermin have low toxicity too, the gelification time using these substances is very long because the slow reaction with chitosan and the final product is very expensive [19,43,44]. These limitations have been

overcome using THPC as linking agent.

Results of mucoadhesiveness studies suggest that the hydrogel is mucoadhesive, due to the interaction between positive charges of chitosan and negative charges of mucin, among other causes. The mucoadhesive properties of chitosan are not lost in spite of the crosslinking.

Finally, it has been shown that gastrointestinal transit time of hydrogels is slower than the reference barium sulphate. The mucoadhesiveness of the hydrogel allows to improve its properties as a controlled release system since the permanence time in the intestine is prolonged. This allows the continuous release of CPT during this time period in the intestinal tract.

## 5. Conclusion

In this research work it has been proposed a new hydrogel drug delivery system that would allow oral treatment with CPT. We have presented an inexpensive, simple, and rapid method to prepare hydrogels using chitosan and THPC as basic components. The hydrogel network was built through the formation of covalent bonding between amine groups of chitosan backbone and hydroxymethyl groups of THPC. We have demonstrated its low toxicity and its potential application as controlled drug release system. The hydrogel mucoadhesive properties allow to prolong the permanence time in the gastrointestinal tract and, consequently, the absorption time that disposes the drug which is released during this period. This system, which controls the antitumor drug release, would provide constant low drug concentrations in small intestine. This would avoid transport saturation (thereby increasing the apparent permeability) and would reduce adverse effects that result from intestinal exposure to high drug concentrations.

## Author contributions

MT. M. M. performed and analyzed experimental studies, G.R.B. performed and analyzed characterization studies of the hydrogel, A.C. supervised chemical study, M.B provided advice on experimental design and data analysis, I.G.A designed *in vitro* and *in vivo* study, contributed to data analysis and conclusions of the study, she is the corresponding author of the work, V.M. design and supervised the study and M.G.A. design and supervised the study. MT. M. M., I.G.A, V.M. and M.G.A. wrote the manuscript. All authors reviewed and commented on the manuscript.

## Funding sources

Authors acknowledge partial financial support to project SAF2016-78756 from MINECO (Spanish Ministry of economy, industry and competitiveness).

## Acknowledgments

Mayte Martínez-Martínez received a grant from the Ministry of Education and Science of Spain (FPU13-01105). The authors acknowledge to Luis Gnecco for pictures.

## References

- [1] L. Bromberg, Intelligent hydrogels for the oral delivery of chemotherapeutics, *Expert Opin. Drug Deliv.* 2 (2005) 1003–1013.
- [2] V.J. O'Neill, C.J. Twelves, Oral cancer treatment: developments in chemotherapy and beyond, *Br. J. Cancer* 87 (2002) 933–937.
- [3] J. Blanchette, N.A. Peppas, Cellular evaluation of oral chemotherapy carriers, *J. Biomed. Mater. Res. A* 72 (2005) 381–388.
- [4] L. Bromberg, Polymeric micelles in oral chemotherapy, *J. Control Release* 128 (2008) 99–112.
- [5] K. Legarza, L.X. Yang, New molecular mechanisms of action of camptothecin-type drugs, *Anticancer Res.* 26 (2006) 3301–3305.
- [6] C.J. Gerrits, M.J. de Jonge, J.H. Schellens, G. Stoter, J. Verweij, Topoisomerase I

- inhibitors: the relevance of prolonged exposure for present clinical development, *Br. J. Cancer* 76 (1997) 952–962.
- [7] J. Fassberg, V.J. Stella, A kinetic and mechanistic study of the hydrolysis of camptothecin and some analogues, *J. Pharm. Sci.* 81 (1992) 676–684.
- [8] A.R. Khan, J.P. Magnusson, S. Watson, A.M. Grabowska, R.W. Wilkinson, C. Alexander, D. Pritchard, Camptothecin prodrug block copolymer micelles with high drug loading and target specificity, *Polym. Chem.* 5 (2014) 5320–5329.
- [9] R. Barreiro-Iglesias, L. Bromberg, M. Temchenko, T.A. Hattton, A. Concheiro, C. Alvarez-Lorenzo, Solubilization and stabilization of camptothecin in micellar solutions of pluronic-g-poly(acrylic acid) copolymers, *J. Control Release* 97 (2004) 537–549.
- [10] M.E. Fox, S. Guillaudeu, J.M.J. Fréchet, K. Jerger, N. Macaraeg, F.C. Szoka, Synthesis and in vivo antitumor efficacy of PEGylated poly(L-lysine) dendrimer – camptothecin conjugates, *Mol. Pharm.* 6 (2009) 1562–1572.
- [11] A.K. Lalloo, F.R. Luo, A. Guo, P.V. Paranjpe, S.H. Lee, V. Vyas, E. Rubin, P.J. Sinko, Membrane transport of camptothecin: facilitation by human P-glycoprotein (ABCB1) and multidrug resistance protein 2 (ABCC2), *BMC Med.* 2 (2004) 16.
- [12] E. Gupta, V. Vyas, F. Ahmed, P. Sinko, T. Cook, E. Rubin, Pharmacokinetics of orally administered camptothecins, *Ann. N.Y. Acad. Sci.* 922 (2000) 195–204.
- [13] J.M. Rosiak, F. Yoshii, Hydrogels and their medical applications, *Nucl. Instr. Meth. Phys. Res. B: Beam Interactions Mater. Atoms* 151 (1999) 56–64.
- [14] T.R. Hoare, D.S. Kohane, Hydrogels in drug delivery: Progress and challenges, *Polymer* 49 (2008) 1993–2007.
- [15] W.E. Hennink, C.F. van Nostrum, Novel crosslinking methods to design hydrogels, *Adv. Drug Deliv. Rev.* 54 (2002) 13–36.
- [16] N. Bhattarai, J. Gunn, M. Zhang, Chitosan-based hydrogels for controlled, localized drug delivery, *Adv. Drug Deliv. Rev.* 62 (2010) 83–99.
- [17] D.P. Speer, M. Chvapil, C.D. Eskelson, J. Ulreich, Biological effects of residual glutaraldehyde in glutaraldehyde-tanned collagen biomaterials, *J. Biomed. Mater. Res.* 14 (1980) 753–764.
- [18] E. Zeiger, B. Gollapudi, P. Spencer, Genetic toxicity and carcinogenicity studies of glutaraldehyde—a review, *Mutat. Res.* 589 (2005) 136–151.
- [19] H.W. Sung, R.N. Huang, L.L. Huang, C.C. Tsai, In vitro evaluation of cytotoxicity of a naturally occurring cross-linking reagent for biological tissue fixation, *J. Biomater. Sci. Polym. Ed.* 10 (1999) 63–78.
- [20] W.A. Reeves, J.D. Guthrie, Intermediate for flame-resistant polymers - reactions of tetrakis(hydroxymethyl)phosphonium chloride, *Ind. Eng. Chem.* 48 (1956) 64–67.
- [21] C. Chung, K.J. Lampe, S.C. Heilshorn, Tetrakis(hydroxymethyl) phosphonium chloride as a covalent cross-linking agent for cell encapsulation within protein-based hydrogels, *Biomacromolecules* 13 (2012) 3912–3916.
- [22] M. Rinaudo, Chitin and chitosan: Properties and applications, *Prog. Polym. Sci.* 31 (2006) 603–632.
- [23] Z.W. Jing, Z.W. Ma, C. Li, Y.Y. Jia, M. Luo, X.X. Ma, S.Y. Zhou, B.L. Zhang, Chitosan cross-linked with poly(ethylene glycol)dialdehyde via reductive amination as effective controlled release carriers for oral protein drug delivery, *Bioorg. Med. Chem. Lett.* 27 (2017) 1003–1006.
- [24] J. Xu, S. Strandman, J.X.X. Zhu, J. Barralet, M. Cerruti, Genipin-crosslinked catechol-chitosan mucoadhesive hydrogels for buccal drug delivery, *Biomaterials* 37 (2015) 395–404.
- [25] P. Mukhopadhyay, K. Sarkar, S. Bhattacharya, A. Bhattacharyya, R. Mishra, P.P. Kundu, pH sensitive N-succinyl chitosan grafted polyacrylamide hydrogel for oral insulin delivery, *Carbohydr. Polym.* 112 (2014) 627–637.
- [26] G.M. El-Mahrouk, M.H. Aboul-Einien, A.I. Makhlouf, Design, optimization, and evaluation of a novel metronidazole-loaded gastro-retentive pH-sensitive hydrogel, *AAPS PharmSciTech* 17 (2016) 1285–1297.
- [27] D. Oltra-Noguera, V. Mangas-Sanjuan, A. Centelles-Sangüesa, I. Gonzalez-García, G. Sanchez-Castaño, M. Gonzalez-Alvarez, V.-G. Casabo, V. Merino, I. Gonzalez-Alvarez, M. Bermejo, Variability of permeability estimation from different protocols of subculture and transport experiments in cell monolayers, *J. Pharmacol. Toxicol. Methods* 71 (2015) 21–32.
- [28] V. Mangas-Sanjuan, I. Gonzalez-Alvarez, M. Gonzalez-Alvarez, V.G. Casabo, M. Bermejo, Modified nonsink equation for permeability estimation in cell monolayers: comparison with standard methods, *Mol. Pharm.* 11 (2014) 1403–1414.
- [29] I. Lozoya-Agullo, M. Zur, A. Beig, N. Fine, Y. Cohen, M. González-Álvarez, M. Merino-Sanjuán, I. González-Álvarez, M. Bermejo, A. Dahan, Segmental-dependent permeability throughout the small intestine following oral drug administration: Single-pass vs. Doluisio approach to in-situ rat perfusion, *Int. J. Pharm.* 515 (2016) 201–208.
- [30] J.T. Doluisio, N.F. Billups, L.W. Dittert, E.T. Sugita, J.V. Swintosky, Drug absorption I: an in situ rat gut technique yielding realistic absorption rates, *J. Pharm. Sci.* 58 (1969) 1196–1200.
- [31] R. Ferrando, T.M. Garrigues, M.V. Bermejo, R. Martin-Algarra, V. Merino, A. Polache, Effects of ethanol on intestinal absorption of drugs: in situ studies with ciprofloxacin analogs in acute and chronic alcohol-fed rats, *Alcohol. Clin. Exp. Res.* 23 (1999) 1403–1408.
- [32] C. Fernandez-Teruel, I. Gonzalez-Alvarez, V.G. Casabo, A. Ruiz-Garcia, M. Bermejo, Kinetic modelling of the intestinal transport of sarafloxacin. Studies in situ in rat and in vitro in Caco-2 cells, *J. Drug Target* 13 (2005) 199–212.
- [33] I. Gonzalez-Alvarez, C. Fernandez-Teruel, V.G. Casabo-Alos, T.M. Garrigues, J.E. Polli, A. Ruiz-Garcia, M. Bermejo, In situ kinetic modelling of intestinal efflux in rats: functional characterization of segmental differences and correlation with in vitro results, *Biopharm. Drug Dispos.* 28 (2007) 229–239.
- [34] I. Lozoya-Agullo, I. Gonzalez-Alvarez, M. Gonzalez-Alvarez, M. Merino-Sanjuan, M. Bermejo, In situ perfusion model in rat colon for drug absorption studies: comparison with small intestine and Caco-2 cell model, *J. Pharm. Sci.* (2015).
- [35] R.W. Kormsmeier, R. Gurny, E. Doelker, P. Buri, N.A. Peppas, Mechanisms of solute release from porous hydrophilic polymers, *Int. J. Pharm.* 15 (1983) 25–35.
- [36] A. Dahan, J.M. Miller, G.L. Amidon, Prediction of solubility and permeability class membership: provisional BCS classification of the world's top oral drugs, *AAPS J.* 11 (2009) 740–746.
- [37] F. Ahmed, V. Vyas, A. Saleem, X.G. Li, R. Zamek, A. Cornfield, P. Haluska, N. Ibrahim, E.H. Rubin, E. Gupta, High-performance liquid chromatographic quantitation of total and lactone 20(S)camptothecin in patients receiving oral 20(S) camptothecin, *J. Chromatogr. B Biomed. Sci. Appl.* 707 (1998) 227–233.
- [38] I. Lozoya-Agullo, M. Zur, A. Beig, N. Fine, Y. Cohen, M. Gonzalez-Alvarez, M. Merino-Sanjuan, I. Gonzalez-Alvarez, M. Bermejo, A. Dahan, Segmental-dependent permeability throughout the small intestine following oral drug administration: Single-pass vs. Doluisio approach to in-situ rat perfusion, *Int. J. Pharm.* 515 (2016) 201–208.
- [39] I. Lozoya-Agullo, M. Zur, N. Fine-Shamir, M. Markovic, Y. Cohen, D. Porat, I. Gonzalez-Alvarez, M. Gonzalez-Alvarez, M. Merino-Sanjuan, M. Bermejo, A. Dahan, Investigating drug absorption from the colon: Single-pass vs Doluisio approaches to in-situ rat large-intestinal perfusion, *Int. J. Pharm.* 527 (2017) 135–141.
- [40] I. Lozoya-Agullo, M. Zur, O. Wolk, A. Beig, I. Gonzalez-Alvarez, M. Gonzalez-Alvarez, M. Merino-Sanjuan, M. Bermejo, A. Dahan, In-situ intestinal rat perfusions for human Fabs prediction and BCS permeability class determination: Investigation of the single-pass vs. the Doluisio experimental approaches, *Int. J. Pharm.* 480 (2015) 1–7.
- [41] I. Candel, E. Aznar, L. Mondragon, C.d.I. Torre, R. Martinez-Manez, F. Sancenon, M.D. Marcos, P. Amoros, C. Guillem, E. Perez-Paya, A. Costero, S. Gil, M. Parra, Amidase-responsive controlled release of antitumoral drug into intracellular media using gluconamide-capped mesoporous silica nanoparticles, *Nanoscale* 4 (2012) 7237–7245.
- [42] H. Schott, Kinetics of swelling of polymers and their gels, *J. Pharm. Sci.* 81 (1992) 467–470.
- [43] B.M. Espinosa-García, W.M. Argüelles-Monal, J. Hernández, L. Félix-Valenzuela, N. Acosta, F.M. Goycoolea, Molecularly imprinted Chitosan – Genipin hydrogels with recognition capacity toward o-Xylene, *Biomacromolecules* 8 (2007) 3355–3364.
- [44] J. Jin, M. Song, D.J. Hourston, Novel Chitosan-based films cross-linked by genipin with improved physical properties, *Biomacromolecules* 5 (2004) 162–168.